NANO LETTERS

pubs.acs.org/NanoLett

Direct Observation of Acoustic Oscillations in InAs Nanowires

Simon O. Mariager,*,† Dmitry Khakhulin,† Henrik T. Lemke,† Kasper S. Kjær,† Laurent Guerin,§ Laura Nuccio,† Claus B. Sørensen,‡ Martin M. Nielsen,† and Robert Feidenhans'l*,†

†Centre for Molecular Movies and ‡Nano-Science Center, Niels Bohr Institute, University of Copenhagen, Universitetsparken 5, 2100 Copenhagen Ø, Denmark and §European Synchrotron Radiation Facility, Grenoble Cedex 38043, France

ABSTRACT Time-resolved X-ray diffraction and optical reflectivity are used to directly measure three different acoustic oscillations of InAs nanowires. The oscillations are excited by a femtosecond laser pulse and evolve at three different time scales. We measure the absolute scale of the initial radial expansion of the fundamental breathing eigenmode and determine the frequency by transient optical reflectivity. For the extensional eigenmode we measure the oscillations of the average radial and axial lattice constants and determine the amplitude of oscillations and the average extension. Finally we observe a bending motion of the nanowires. The frequencies of the eigenmodes are in good agreements with predictions made by continuum elasticity theory and we find no difference in the speed of sound between the wurtzite nanowires and cubic bulk crystals, but the measured strain is influenced by the interaction between different modes. The wurtzite crystal structure of the nanowires however has an anisotropic thermal expansion.

KEYWORDS InAs, nanowires, coherent phonons, acoustic oscillations, X-ray scattering

Acoustic oscillations, also known as coherent acoustic phonons, in nanowires are of interest in practical applications as well as in fundamental research. Metal nanowires are considered for sensing, photonics, and catalysis, while semiconductor nanowires are proposed as tools for sensitive force and mass detection.[1−4] In general acoustic oscillations could prove an easy way to determine the geometry of nanostructures[5] and measure their mechanical properties.[6−9] Nanostructures also provide a possibility to study acoustic phonons by using the dimension of the nanostructure to control the length scale of the phonon wavevector. A variety of techniques has been applied to study acoustic vibrations in nanowires. Relatively slow bending modes in cantilevers have been filmed by scanning electron microscopy (SEM)[8,10] and transmission electron microscopy[7] and in real space by 4D electron microscopy,[11] and atomic force microscopes have been used to bend wires.[9] Most investigations were done using optical methods such as Raman spectroscopy,[5] transient absorption, and scattering[7,12−15] or optical interferometry.[16,17] Optical methods are superior for ease of application and availability, but assignment of the measured frequency or period to a specific mode relies on an interpretation based on continuum elasticity theory applied to the anisotropic crystal systems. Though the displacement of a mode is not determined, the agreement with theory is good and has been validated by comparison to finite element calculations.[5,6] Studies on nanowires however find both decreasing (GaN,[7] Cr[18]), increasing (ZnO[10]) and constant (Ge,[8] Au,[12] Bi[14]) elastic modulus with decreasing wire diameter. While these results need not be contradicting, techniques which can investigate and confirm the assumptions made in continuum elasticity theory, by directly measuring the atomic motion of nanostructures, are pivotal in the fundamental research underlying practical applications. One method which directly measures changes in the crystal lattice is time-resolved X-ray diffraction, a technique which has previously been used to study coherent phonons in superlattices.[19] In this Letter we briefly review the various classes of eigenmodes of a thin elastic rod and then present the results of time-resolved X-ray experiments performed on InAs nanowires. Finally we discuss the evolution of the nanowire motion when excited by ultrafast laser pulses through three different acoustic oscillations and the eventual breaking of the wires.

A thin rod (length $L \gg$ radius R) considered in continuum elastic theory possesses several classes of acoustic eigenmodes. The three modes of relevance for this study are (i) the breathing mode corresponding to oscillations in the radial direction, (ii) the extensional mode corresponding to an axial extension accompanied by a small radial contraction, and (iii) the bending mode corresponding to a bending of the wire. For an isotropic rod the frequencies are expressed in terms of Young's modulus, the mass density, and Poisson's ratio ν, but for an anisotropic crystal we substitute by the relevant speeds of sound. The periods of oscillation of the fundamental breathing, extensional, and bending modes for a crystal nanowire with one fixed and one free end are given as[6,20]

* To whom correspondence should be addressed, som@fys.ku.dk and robert@fys.ku.dk.

Received for review: 03/5/2010
Published on Web: 05/27/2010

DOI: 10.1021/nl100798y | *Nano Lett.* **2010,** *10,* 2461–2465

$$T_{\mathrm{br}} = \frac{2\pi}{\tau_{\mathrm{br},n}}\frac{R}{v_{\mathrm{R}}}, \quad T_{\mathrm{ext}} = \frac{4L}{v_{\parallel}}, \quad T_{\mathrm{ben}} = \frac{2\pi L^2}{\tau_{\mathrm{ben},n} v_{\parallel}}\sqrt{\frac{S}{I}} \tag{1}$$

v_R is the speed of sound for a longitudinal wave along the radial axis and $\tau_{br,n}$ is a constant given by an eigenvalue equation dependent upon Poisson's ratio.[6] $v_{\parallel}$ is the speed of sound for a longitudinal wave traveling along the axial direction of the wire assuming that the axial direction corresponds to a symmetry axis of the crystal. For the fundamental bending mode $\tau_{ben,1} = 3.517$ is given by the boundary conditions, S is the cross-sectional area, and I is the moment of inertia for a rotation of the cross section. The InAs wires introduced below (Figure 1) all have a hexagonal cross section which results in $(S/I)^{1/2} = (24/5)^{1/2}/R$ independent of the rotational axis. The basic time scales for the fundamental eigenmodes are thus given by the ratios of the radius and the length of the wire to the speed of sound with typical time scale for nanowires from tens of picoseconds in the breathing mode to hundreds of nanoseconds in the bending mode.

The spatial dependence of the strain in the fundamental extensional mode in the limit $L \gg R$ is given as[21]

$$\vec{u}_{\mathrm{ext}}(r,z) \propto \sin\left(\frac{\pi z}{2L}\right)\vec{z} - \nu\frac{\pi r}{2L}\cos\left(\frac{\pi z}{2L}\right)\vec{r}$$

where $\vec{z}$ and $\vec{r}$ are unit vectors in the direction along and perpendicular to the wire assuming cylindrical symmetry. From this equation it follows that the ratio of the average axial and radial expansion is given by Poisson's ratio as $-1/\nu$.

The InAs nanowires were grown along the surface normal of an InAs (111) substrate by molecular beam epitaxy. They consist mainly of the hexagonal wurtzite structure and have a hexagonal cross section with radius $r = 49 \pm 7$ nm and length $L = 4.4 \pm 0.7$ μm (Figure 1).[22] The time-resolved X-ray diffraction experiments were conducted at ID09B at the European Synchrotron Radiation Facility (ESRF), with preliminary experiments performed at sector 7 at the Advanced Photon Source (APS). A time resolution of approximately 100 ps is achieved by mechanically selecting the radiation from a single bunch in the storage ring at a repetition rate of 986.3 Hz in phase with a Ti:sapphire pump laser delivering 800 nm 100 fs pump pulses (spot size 0.39 $\times$ 0.66 mm^2).[23] The diffraction signal from an entire forest of nanowires was obtained as a series of laser-on/laser-off images and consisted of 2D images of Bragg peaks, from which the peak shifts, and subsequently the change in average lattice constants can be extracted as a function of time delay between the pump and probe pulses. For the same sample we also measured the optical reflectivity transients in a two-color femtosecond pump–probe setup

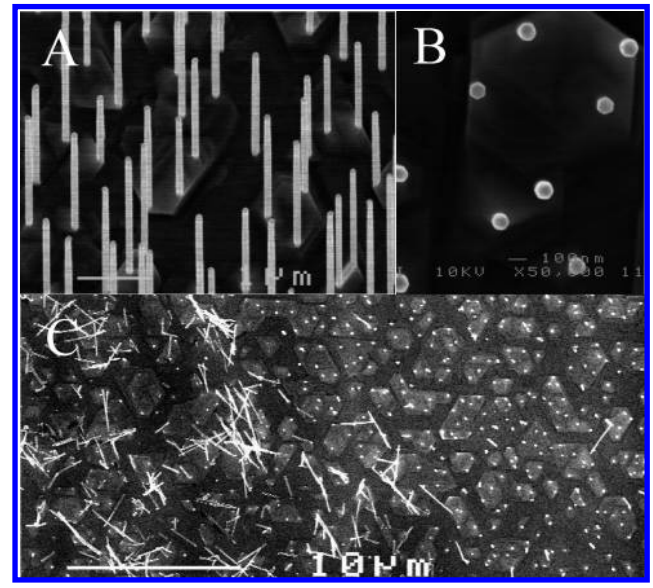

FIGURE 1. SEM images of InAs nanowires seen at an angle of 20° (A) and showing the hexagonal facets from a top view (B). The lower image (C) shows a region of wires broken at high laser power.

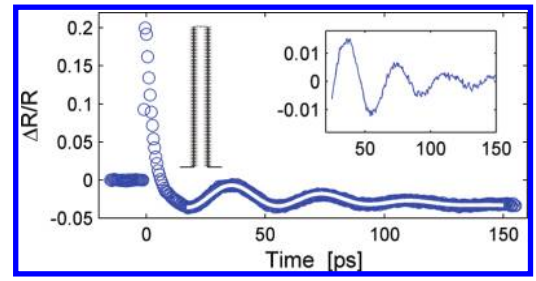

FIGURE 2. Breathing mode. Transient laser reflectivity measured on the InAs nanowires. The white line is a fit to the data. The inserts show the oscillatory part of the signal, and a schematic drawing of the bending mode.

based on a Ti:sapphire laser. White light continuum generated in a 2 mm thick sapphire was used as the probe and the fundamental radiation (800 nm) as pump with a pump fluence of 6 mJ/cm^2.

In this experiment the laser pulse excites electron–hole pairs in the wires which subsequently decay via coupling to acoustic phonons resulting in a heating of the nanowire. The change in lattice temperature can excite acoustic oscillations through two processes: (i) A nonuniform temperature distribution gives rise to thermal stress launching strain waves.[24] (ii) The rise in temperature increases the equilibrium lattice constants and as the electron–hole relaxation is much faster than the acoustic eigenmodes, the lattice is suddenly out of equilibrium and acoustic oscillations are initiated. This constitutes a displacive excitation.[25]

Figure 2 shows the optical transient reflectivity measured for the first 150 ps after excitation. The fast initial (<1 ps) rise can be assigned to the creation of excited electron–hole pairs, while the signal later shows an oscillation with a period of 38.3 $\pm$ 0.1 ps, in good agreement with the predicted value of 35 ps for the breathing mode, found by using a calculated

DOI: 10.1021/nl100798y | Nano Lett. 2010, 10, 2461–2465

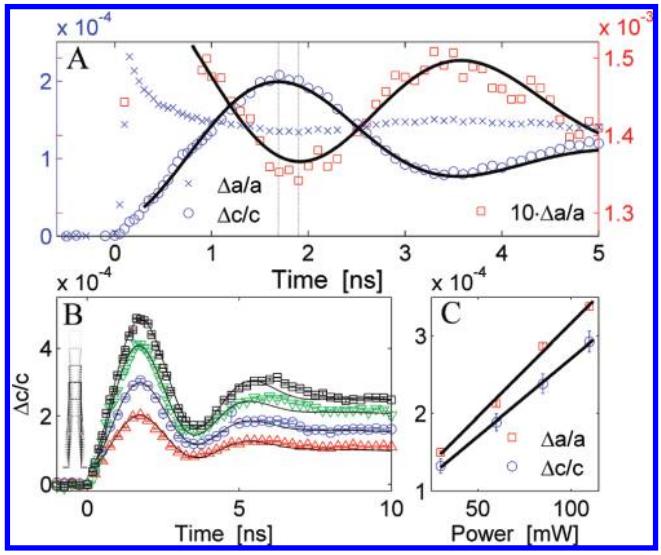

FIGURE 3. Extensional mode. (A) Relative change in lattice constants *a* (crosses) and *c* (circles) as a function of time. The motion in the axial lattice constant *a* has also been amplified 10 times (squares, right *y* axis) for easier comparison. The vertical lines serve as guides to the eye for the phase shift in the first extrema. The solid lines are fit to the data. (B) Relative change in the axial lattice constant *c* at powers of 30 (triangles), 60 (circles), 85 (down-pointing triangles), and 110 mW (squares) including fits to the data. (C) Average extension as a function of power.

Poisson's ratio of 0.22 giving $\tau_{br,1} = 2.04$[6] and $v_{[101],c} =$ 4.28km/s from cubic InAs data.[26,27] Hence, we assign the transient reflectivity data for times larger than about 5 ps to the breathing mode in the radial direction. At slightly longer time scales, we see the extensional mode. In Figure 3A we show the relative change, as measured by time-resolved X-ray diffraction, in the average hexagonal lattice constants *a* (radial) and *c* (longitudinal) during the first 5 ns after excitation. The lower temporal resolution does not allow us to resolve the breathing mode, but the first data points (<100 ps) reveal a purely radial motion with a relative increase in radius of the wire of 2.4×10^{-4} or 12 pm and no change in the length of the wire. If we make the assumption that the change in optical reflectivity is linear with strain, this can be used to calibrate the values from Figure 2, where the amplitude of the oscillations in the breathing mode is then ~8 pm corresponding to a strain in the radial lattice constant of $\Delta a/a = 1.6 \times 10^{-4}$. On a time scale of 2 ns axial oscillations set in corresponding to the fundamental extensional mode, with the radial distortion Δa and the longitudinal distortion Δc oscillating out of phase as shown in Figure 3A. The fact that the oscillations start out at an extremum is the signature of a displacive excitation. In Figure 3B we show the evolution in Δc up to 10 ns for different laser powers. Assuming the oscillating signal corresponds to the single damped fundamental eigenmode, the data in parts A and B of Figure 3 have been fitted with a function of the type $A \exp(-t/b) + C \exp(-(t/\tau)^2) \cos(\omega t + \phi)$. The fit parameters from Figure 3B reveal that the period, damping, and phase are independent of the laser power, while the amplitude (parameter *C*) and background (parameter *A*) scale linearly with laser power below the damage threshold. The fit shown in parts A and B of Figure 3 gives a period of 3.86 ± 0.14 ns (95% confidence bounds), corresponding to a speed of sound of 4.50 ± 0.18km/s, which is in good agreement with the corresponding value from cubic bulk InAs of $v_{[111],c} =$ 4.41 km/s.[26] In Figure 3A the radial signal has been amplified 10-fold for easier comparison with the axial part. It is evident and highlighted by vertical lines serving as guides to the eye that the first minimum of the oscillations in *a* is slightly delayed compared to the first maximum in *c*. This is not predicted in the description of the extensional mode by continuum elasticity theory but can be attributed to the interaction between the breathing and extensional modes. The fitted functions indicate a general delay of the radial oscillation of 85 ps, but careful measurements of more periods than the two visible in Figure 3C are needed to confirm this. Such a phase lag would be reasonable if the axial extension induces the radial contraction and the time scale is consistent with the period of the breathing mode. The amplitude of the oscillation in lattice constant *c* corresponds to a change in wire length of only 4.8 Å, and the ratio of the oscillation amplitudes of *a* and *c* gives a Poisson's ratio of 0.10 ± 0.05, in poor agreement with the nominal value of 0.22. This could also be due to the simplified derivation of the eigenmode, in which the initial assumption is that no radial motion occurs, in stark contrast to our dynamic system in which the wires are expanded by the breathing mode during the onset of the extensional mode. It is clear that a theoretical approach which also considers the interaction between the various acoustic eigenmodes is needed to accommodate the detailed features of the strain observed here. The fit parameter *A* gives the average change in lattice constants *a* and *c* and is plotted as a function of power in Figure 3C. The ratio of the gradients gives the ratio of the lattice thermal expansion coefficients as $\alpha_a/\alpha_c = 1.21$. While bulk InAs as a cubic structure shows no such anisotropy for different crystallographic directions other wurtzite semiconductors as InN and GaN show similar ratios for the thermal expansions along [100] and [001] hexagonal directions.[28] For an order of magnitude estimate we anyway use the thermal expansion coefficient of bulk InAs of 4.52×10^{-6} K^{-1} and find a temperature rise of ~30 K at the lowest laser power. This temperature rise is consistent with the laser power of 30 mW confirming the magnitude of the calculated strains. Figure 3B shows how the oscillations decay after two periods. This decay is best described by a function $\exp(-(t/\tau)^2)$, which is expected for the decay due to nanowires of different lengths having different fundamental frequencies.[29] In the second period the fit of the decay is not adequately described by the simple model. Factors as the Au particle on top of the wires and coupling to the substrate, both of which are ignored, serve to explain this.

In Figure 4 we show the evolution in the position of the [102] wurtzite Bragg point in reciprocal lattice coor-

DOI: 10.1021/nl100798y | *Nano Lett.* **2010,** *10,* 2461–2465

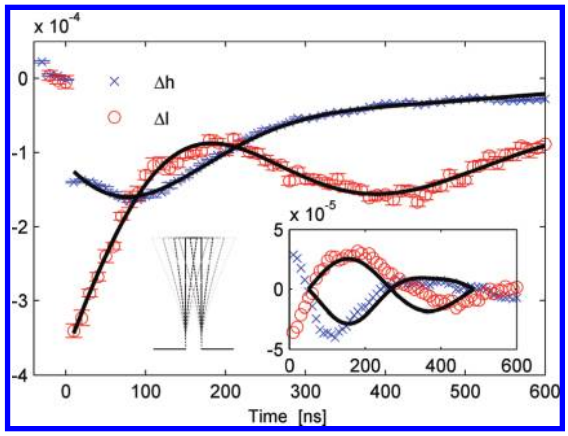

FIGURE 4. Bending mode. Absolute change in reciprocal space coordinates *h* and *l* including fits to the data. Insert: Oscillatory part of the motion and simulation (solid lines) of the scattering from a bending wire.

dinates up to 600 ns. The data show an oscillatory motion which is highlighted in the insert (data with the exponential background subtracted). Note that the bending mode displayed in Figure 4 does not start with zero displacement in reciprocal space as the wires are already radially and axially expanded when the bending motions start, and since the wires act as a dispersive medium for bending waves, the excitation of higher modes will lead to a nonperiodic signal. The data were fitted with the same function as used for the extensional mode, and the two periods of the fits are ~440 ± 84 and ~523 ± 61 ns for the radial and axial motion, respectively. They are somewhat higher from the theoretically expected fundamental bending eigenmode of 343 ns calculated from eq 1. While we thus do not excite the fundamental eigenmode, we confirm that the motion does correspond to a bending by calculating the lattice sum of the off-planar [102] wurtzite Bragg point for a bending wire. The nanowire bends in the laser scattering plane (coinciding with the X-ray incoming beam) and initially bends away from the laser. We use the expression for the bending of a small part of an elastic rod extended to the entire nanowire.[20] The result, damped to match the data, is shown with solid lines in the insert in Figure 4. The qualitative agreement between data and calculation is good. The phase of the signal in the reciprocal coordinates h and l, as well as the relative amplitudes matches well. Δl corresponds to a pure cosine signal, while Δh deviates from the pure cosine in the second half of the period, when the wire bends toward the laser and X-ray sources. We emphasize that no other bending motion reproduces the results, and we conclude that a bending occurs in the laser-scattering plane. The simulations indicate a radius of curvature of the bending with a magnitude on the order of ~1000L, in agreement with the small displacements found for the extensional mode.

On the basis of the laser and X-ray data presented, we propose the following interpretation of the nanowires motion. Initially heated by the fast laser pulse, the dimensions of the wire only allow a radial expansion giving rise to the breathing mode. At the same time the extensional mode is launched with some delay between the axial and radial motions, and finally a bending motion is initiated. We thus see three different acoustic modes excited in the InAs nanowires by a single laser pulse. The concept of displacive excitations provides a simple explanation of the breathing and extensional modes but can only launch symmetry conserving modes. We thus speculate that the strain waves rising from the uneven heating of the wire launches a bending motion in the laser-scattering plane, with the excitation resulting in a motion far from the fundamental eigenmode. At higher laser powers[30] the X-ray signal disappears and the sample is visibly damaged. Figure 1C shows a SEM image of a damaged region which reveals that the wires have broken off the substrate. Considering the small vibration amplitudes, the wires in this study can only sustain a low strain before fracturing, in contrast to previous studies on Ge wires.[8] The result is however not surprising as the InAs nanowires contain numerous stacking faults extending across the entire cross section of the wire.

In conclusion, we show that time-resolved X-ray diffraction experiments can reveal detailed descriptions of the vibrational modes of nanostructures, and the data presented here show three different acoustic vibrations excited in the nanowires by a single laser pulse. From the X-ray data for the extensional mode, we extract absolute values for the amplitude of oscillations and average extension of the wires and indicate a phase lack between radial and longitudinal oscillations. The speeds of sound, and hence the elastic moduli, of the wurtzite InAs nanowires agree with those of bulk cubic InAs, but the wurtzite nanowires have anisotropic thermal expansion coefficients. By measuring the actual motion of the oscillations, we assign these to three eigenmodes predicted by continuum elasticity theory, and find a good agreement between measured and calculated periods; supporting the use of purely optical methods to determine frequency or period. Features of the strain, such as the delay between radial and axial extrema in the first period of the extensional eigenmode and the low poisson's ratio, however show that a precise theoretical description of the strain must take into account the interaction of the eigenmodes which overlap in time in order to fully understand the nanowires' mechanical behavior.

Acknowledgment. We wish to thank the staff at beamline ID09b of the ESRF, in particular Michael Wulff, for their invaluable help and assistance. We also thank the staff at sector 7 of APS for their help and assistance. Finally we thank Joanna Eriksen for participating in the measurements of the damage threshold of the nanowires. The work was

DOI: 10.1021/nl100798y | *Nano Lett.* **2010,** *10,* 2461--2465

supported by the Danish Natural Science Council through DANSCATT and by the Danish National Science Foundation.

Supporting Information Available. Additional details on the nanowire growth process, the laser setup, and the time-resolved X-ray technique. This material is available free of charge via the Internet at http://pubs.acs.org.

REFERENCES AND NOTES

(1) Ekinci, K. L.; Roukes, M. L. *Rev. Sci. Instrum.* **2005**, *76*, No. 061101.
(2) Yan, R.; Gargas, D.; Yang, P. *Nat. Photonics* **2009**, *3*, 569.
(3) Hochbaum, A. I.; Yang, P. *Chem. Rev.* **2010**, *110*, 527.
(4) Xia, Y.; Yang, Y.; Sun, Y.; Wu, Y.; Mayers, B.; Gates, B.; Yin, Y.; Kim, F.; Yan, H. *Adv. Mater.* **2003**, *15*, 353.
(5) Lange, H.; Mohr, M.; Artemyev, M.; Woggon, U.; Thomsen, C. *Nano Lett.* **2008**, *8*, 4614.
(6) Hu, M.; Wang, X.; Hartland, G. V.; Mulvaney, P.; Juste, J. P.; Sader, J. E. *J. Am. Chem. Soc.* **2003**, *125*, 14925.
(7) Nam, C.-Y.; Jaroenapibal, P.; Tham, D.; Luzzi, D. E.; Evoy, S.; Fischer, J. E. *Nano Lett.* **2006**, *6*, 153.
(8) Smith, D. A.; Holmbert, V. C.; Lee, D. C.; Korgel, B. A. *J. Phys. Chem. C* **2008**, *112*, 10725.
(9) Wong, E. W.; Sheehan, P. E.; Lieber, C. M. *Science* **1997**, *277*, 1971.
(10) Chen, C. Q.; Shi, Y.; Zhang, Y. S.; Zhu, J.; Yan, Y. J. *Phys. Rev. Lett.* **2006**, *96*, No. 075505.
(11) Flannigan, D. J.; Samartzis, P. C.; Yurtsever, A.; Zewail, A. H. *Nano Lett.* **2009**, *9*, 875.
(12) Zijlstra, P.; Tchebotareva, A. L.; Chon, J. W. M.; Gu, M.; Orrit, M. *Nano Lett.* **2008**, *8*, 3493.
(13) Owrutsky, J. C.; Pomfret, M. B.; Brown, D. J. *J. Phys. Chem. C* **2009**, *113*, 10947.
(14) Kolomenskii, A. A.; Jerebtsov, S. N.; Liu, H.; Zhang, H.; Ye, Z.; Luo, Z.; Wu, W.; Schuessler, H. A. *J. Appl. Phys.* **2008**, *104*, 103110.16. Chen, C. Q.; Shi, Y.; Zhang, Y. S.; Zhu, J.; Yan, Y. J. *Phys. Rev. Lett.* **2006**, *96*, No. 075505.
(15) Yu, P.; Tang, J.; Sheng-Hsien, L. *J.Phys.Chem.C* **2008**, *112*, 17133.
(16) Nichol, J. M.; Hemesath, E. R.; Lauhon, L. J.; Budakian, R. *Appl. Phys. Lett.* **2008**, *93*, 193110.
(17) Belov, M.; Quitoriano, N. J.; Sharma, S.; Hiebert, W. K.; Kamins, T. I.; Evoy, S. *J. Appl. Phys.* **2008**, *103*, No. 074304.
(18) Nilsson, S. G.; Borrisé, X.; Montelius, L. *Appl. Phys. Lett.* **2004**, *85*, 3555.
(19) Bargheer, M.; Zhavoronkov, N.; Gritsai, Y.; Woo, J. C.; Kim, D. S.; Woerner, M.; Elsaesser, T. *Science* **2004**, *306*, 1771.
(20) Landau, L. D.; Pitaevskii, L. P.; Lifshitz, E. M.; Kosevich, A. M. Theory of Elasticity, 3rd ed.; Butterworth-Heinemann: Oxford and New York, 1986.
(21) There appears to be an error in formula 3 in ref 6, where sin and cos have been interchanged.
(22) Mariager, S. O.; Lauridsen, S. L.; Dohn, A.; Bovet, N.; Sørensen, C. B.; Schlepütz, C. M.; Willmott, P. R.; Feidenhans'l, R. *J. Appl. Crystallogr.* **2009**, *42*, 369.
(23) Cammarata, M.; et al. *Rev. Sci. Instrum.* **2009**, *80*, No. 015101.
(24) Thomsen, C.; Grahn, H. T.; Maris, H. J.; Tauc, J. *Phys. Rev. B* **1986**, *34*, 4129.
(25) Bucksbaum, P. H. *Science* **2004**, *306*, 1693.
(26) Burenkov, Y. A.; Davydov, S. Y.; Nikanorov, S. P. *Sov. Phys. Solid State* **1975**, *17*, 1446.
(27) Zhang, J.-M.; Zhang, Y.; Xu, K.-W.; Ji, V. *J. Phys. Chem. Solids* **2007**, *68*, 503.
(28) Zubrilov, A. In *Properties of Advanced SemiconductorMaterials GaN, AlN, InN, BN, SiC, SiGe*; Levinshtein, M. E., Rumyantsev, S. L., Shur, M. S., Eds.; John Wiley & Sons: New York, 2001; pp 49–66.
(29) Hartland, G. V. *J. Chem. Phys.* **2002**, *116*, 8048.
(30) We did not determine the damage threshold, but a laser power of 199 mW reduced the X-ray signal by 50% in 1 s and visibly damaged the sample.

DOI: 10.1021/nl100798y | *Nano Lett.* **2010,** *10,* 2461--2465